Grafting Nitrilotriacetic Groups onto Carboxylic Acid-Terminated Self-Assembled Monolayers on Gold Surfaces for Immobilization of Histidine-Tagged Proteins

Jungkyu K. Lee,[†] Yang-Gyun Kim,[‡] Young Shik Chi,[†] Wan Soo Yun,[§] and Insung S. Choi*[,†]

Department of Chemistry and School of Molecular Science (BK21), Center for Molecular Design and Synthesis, Korea Advanced Institute of Science and Technology (KAIST), Daejeon 305-701, Korea, Department of Biochemistry, College of Medicine, Chung-Ang University, 221 Heuksuk-dong, Dongjak-gu, Seoul 156-756, Korea, and Electronic Device Group, Korea Research Institute of Standards and Science (KRISS), Daejeon 305-600, Korea

Received: December 12, 2003; In Final Form: March 30, 2004

In this paper, we report a common intermediate method to present nitrilotriacetic acid (NTA) groups on gold surfaces for immobilizing His-tagged proteins onto the surfaces, and a full characterization of self-assembled monolayers (SAMs) terminating in carboxylic acids [$HS(CH_2)_{15}COOH$ (C15-COOH), $HS(CH_2)_{11}(OCH_2CH_2)_3OCH_2COOH$ (EG3-COOH), and $HS(CH_2)_{11}(OCH_2CH_2)_5OCH_2COOH$ (EG5-COOH)] and coupling reactions of an NTA-containing primary amine [(1S)-*N*-(5-amino-1-carboxypentyl)iminodiacetic acid; NTA−NH_2] with the carboxylic acid on surfaces. The lateral packing densities of the COOH-terminated SAMs were calculated to be 4.32 (for C15-COOH), 3.49 (for EG3-COOH), and 2.65 (for EG5-COOH) molecules/nm^2. The packing densities were decreased by incorporating a relatively flexible ethylene glycol (EG) group into the backbone of alkanethiols and increasing the number of the EG groups in the backbone of alkanethiols. The NTA group was then attached by coupling NTA−NH_2 with the COOH group on the surfaces, followed by a Ni(II) complexation. The coupling reaction was characterized by FT-IR spectroscopy, ellipsometry, and XPS, and the coupling efficiency ("yield") was estimated by comparing the experimentally determined N 1s to S 2p (N/S) ratio of XPS data with the N/S ratio calculated for the functionalization of the SAMs presenting NTA-Ni(II): the coupling yields were 30% (for C15-COOH) and 25% (for EG3-COOH and EG5-COOH). Preliminary experiments on the binding of His-tagged proteins onto the surfaces were also performed.

Introduction

Chemical reactions on solid surfaces are of importance for the fundamental understanding of interfacial phenomena[1−5] and for a wide variety of technological applications, including microarrays,[6] (bio)sensors,[7,8] catalysis,[9] and biocompatible coating.[10−13] In the area of protein microarrays, it is the first and crucial step for the functional and structural study of molecular interactions between proteins and ligands on surfaces to immobilize proteins onto surfaces in the controlled and oriented way.[14−16] The orientation-controlled immobilization of proteins and other biomolecules onto surfaces allows enhanced/maximized interactions between the immobilized biomolecules and ligands, and in this respect various chemistry- and biology-based[17,18] methods have been developed utilizing biotin-streptavidin interaction,[19−22] antigen−antibody interaction,[23−25] histidine-nickel interaction,[26−35] and protein−ligand (or protein−protein) interaction.[36−41]

Self-assembled monolayers (SAMs) on gold have been utilized as model surfaces for studying biological phenomena and as platforms for the applications mentioned above.[42−44] Two methods are currently used for the generation of surfaces or surface films presenting biomolecules or ligands based on SAMs on gold: (1) direct method, where any desired molecules (usually alkanethiols presenting biomolecules or ligands for the formation of SAMs on gold) are designed and synthesized separately in solution, and the synthesized molecules are assembled on gold surfaces;[36] and (2) common intermediate method, where SAMs are formed on gold surfaces and the SAM-forming thiols contain (potentially) reactive chemical groups at their tail ends. Carboxylic acid groups are usually utilized for an amide bond formation via acid chloride,[45,46] interchain anhydride,[47,48] pentafluorophenyl ester,[49] or *N*-hydroxysuccimide (NHS)-activated carboxylic acid.[50−52] Compared with the direct method, the common intermediate method does not require cumbersome separate synthesis of molecules in solution and could easily be applied to the generation of micro- and nanoarrays with the existing techniques for generating micro- and nanopatterns such as spotting,[53] ink-jet printing,[54,55] micro-[56] and nanocontact printing,[57−59] dip-pen nanolithography,[60−62] and other scanning probe microscope (SPM)-based methods.[30,63] Another disadvantage of the direct method is a limited compatibility of functional groups (especially for SAMs of siloxanes on glass or silicon oxide surfaces). In this paper, we studied an amide coupling reaction of a nitrilotriacetic acid (NTA)-containing amine with three different carboxylic acid-terminated SAMs on gold with varied length and flexibility of the thiols (C15-COOH, EG3-COOH, and EG5-COOH) (For the structures, see Figure 1). The SAMs of C15-COOH, EG3-COOH, and EG5-COOH were fully characterized, and the lateral packing densities were estimated by X-ray photoelectron spectroscopy (XPS). The coupling efficiency was deduced from spectroscopic methods, and a preliminary study on the immobilization of proteins was performed by surface plasmon resonance (SPR) spectroscopy. In addition, effects of the functionality and flexibility of the linker groups of the SAM-forming thiols on bio-specific immobilization of and nonspecific adhesion of proteins were also studied.

* To whom correspondence should be addressed. Tel: +82-42-869-2840. Fax: +82-42-869-2810. E-mail: ischoi@kaist.ac.kr.
[†] KAIST.
[‡] Chung-Ang University.
[§] KRISS.

10.1021/jp0378236 CCC: $27.50
Published on Web 05/07/2004

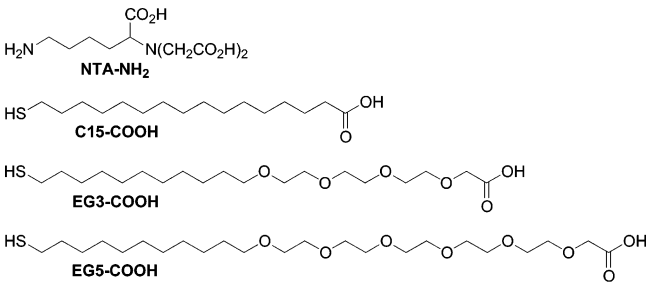

Figure 1. Molecular structures of NTA-NH_2 and three COOH-terminated thiols (C15-COOH, EG3-COOH, and EG5-COOH) used in this study.

NTA has primarily been used for immobilized metal ion affinity chromatography (IMAC), where NTA is covalently bonded to chromatography resins and is usually coordinated with a divalent metallic ion, Ni(II).[64] Upon the coordination with Ni(II), three carboxylate groups and a tertiary amine group of NTA are used leaving two binding sites of Ni(II) accessible to further binding. For the protein purification, proteins are genetically engineered to present a sequence of six histidines (His tag) at their extremity: the His tag strongly binds to the NTA-Ni(II) complex. There have been reports on the direct method for forming SAMs presenting the NTA-Ni(II) group.[65,66] In this study, we investigated a common intermediate method for the generation of NTA-Ni(II)-presenting surfaces on gold: we coupled an NTA-containing amine [(1S)-*N*-(5-amino-1-carboxypentyl)iminodiacetic acid; NTA-NH_2] with the COOH group on gold, followed by a Ni(II) complexation for the immobilization of His-tagged proteins onto surfaces.

Experimental Section

Materials. 1-Eicosanethiol (C20SH) and 1-docosanethiol (C22SH) were synthesized by following the reported procedure.[67] 1-Undecanethiol (C12SH), 1-hexadecanethiol (C16SH), 1-octadecanethiol (C18SH), and 16-mercaptohexadecanoic acid (C15-COOH) were purchased from Aldrich. All solvents and reagents were purchased from Aldrich and used without further purification.

Synthesis. *(a) 23-Mercapto-3,6,9,12-tetraoxatricosanoic Acid (EG3-COOH).* The synthesis of EG3-COOH is outlined in Figure 2. To a THF solution (30 mL) of tri(ethylene glycol) (7.16 g, 47.7 mmol) was added NaH (381.2 mg of 60% suspension in oil, 9.53 mmol) at 0 °C. The resulting mixture was stirred at 0 °C for 30 min and then heated at 80 °C for 2 h under an argon atmosphere. When the solution turned to dark brown, 11-bromo-1-undecene (2 g, 8.58 mmol) was added to the solution, and the resulting mixture was stirred at 80 °C for 12 h. The resulting solution was cooled to room temperature and extracted with hexane (500 mL). The hexane layer was washed with deionized (DI) water, dried over $MgSO_4$, concentrated in vacuo, and purified by column chromatography (elution with hexane:ethyl acetate = 2:1) to give the product **1** in 80% yield. ^{1}H NMR (300 MHz, $CDCl_3$): δ 5.73 (m, 1H), 4.87 (m, 2H), 3.53 (m, 12H), 3.40 (t, 2H), 2.70 (t, 1H), 2.05 (q, 2H), 1.53 (q, 2H), 1.25 (br m, 12H).

To a solution of **1** (2.13 g, 7.05 mmol) in dry DMF (5 mL) was added NaH (253.7 mg of 60% suspension in oil, 10.6 mmol) at 0 °C. The mixture was stirred at 0 °C for 10 min, and *tert*-butyl bromoacetate (2.75 g, 14.1 mmol) was added in one portion. The resulting mixture was stirred at room temperature for 12 h. The crude product was extracted by ethyl acetate (100 mL), dried over $MgSO_4$, and concentrated in vacuo. Column chromatography (elution with 3% MeOH in CH_2Cl_2) afforded the product **2** (2.05 g, 70%). ^{1}H NMR (300 MHz, $CDCl_3$): δ 5.73 (m, 1H), 4.87 (m, 2H), 3.97 (s, 2H), 3.53 (m, 12H), 3.40 (t, 2H), 2.01 (q, 2H), 1.53 (m, 2H), 1.42 (s, 9H), 1.23 (br m, 12H).

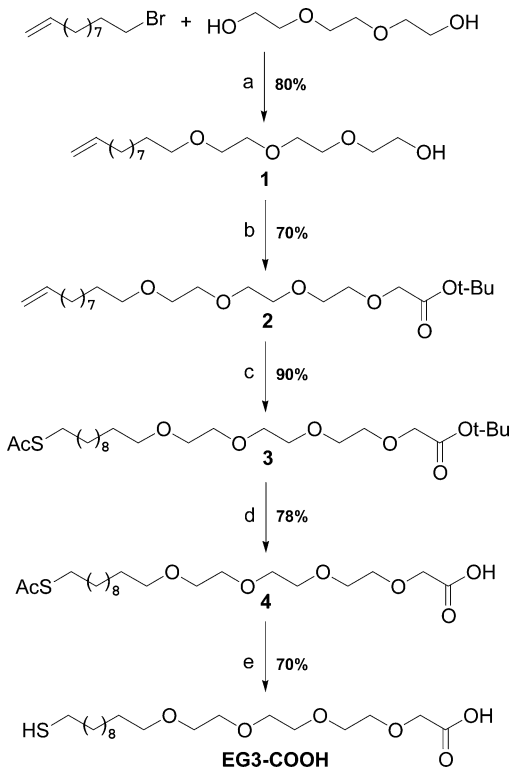

Figure 2. Synthesis of EG3-COOH. (a) NaH, THF; (b) NaH, DMF then $BrCH_2COO$*t*-Bu; (c) TFA, CH_2Cl_2; (d) CH_3COSH, ABCV, THF with UV irradiation; (e) $NaOCH_3$, MeOH.

A mixture of **2** (1.4 g, 3.48 mmol), thioacetic acid (5 mL, 69.6 mmol) and 4,4'-azobis(4-cyanovaleric acid) (ABCV) (150 mg) in THF (40 mL) was irradiated by UV (253.7 nm). After 4 h, additional ABCV (150 mg) was added, and the irradiation was continued for 6 h. The mixture was concentrated in vacuo and purified by column chromatography (elution with 5% MeOH in CH_2Cl_2) to give the thioacetate **3** (1.5 g, 90%).^{1}H NMR (300 MHz, $CDCl_3$): δ 3.99 (s, 2H), 3.53 (m, 12H), 3.40 (t, 2H), 2.83 (t, 2H), 2.29 (s, 3H), 1.53 (m, 2H), 1.42 (s, 9H), 1.23 (br m, 12H).

To a CH_2Cl_2 solution of **3** (1.1 g, 2.23 mmol) was added trifluoroacetic acid (30 mL), and the mixture was stirred at room temperature for 3 h. After the concentration in vacuo and the purification by column chromatography (elution with 10% MeOH in CH_2Cl_2) the product **4** was obtained (759 mg, 78%).^{1}H NMR (300 MHz, $CDCl_3$): δ 3.91 (s, 2H), 3.53 (m, 12H), 3.40 (t, 2H), 2.83 (t, 2H), 2.30 (s, 3H), 1.53 (m, 2H), 1.23 (br m, 12H).

The compound **4** (200 mg, 0.458 mmol) was dissolved in absolute MeOH (10 mL), and the solution was cooled to 0 °C. NaOMe (298.2 mg of 25 wt. % solution in methanol, 1.38 mmol) was added, and the resulting mixture was stirred at 0 °C for 30 min. The mixture was neutralized with 1 N HCl and concentrated in vacuo. The product, EG3-COOH (180 mg, 70%), was purified by column chromatography (elution with 10% MeOH in CH_2Cl_2). ^{1}H NMR (300 MHz, $CDCl_3$): δ 4.18 (s, 2H), 3.54 (m, 12H), 3.45 (t, 2H), 2.51 (q, 2H), 1.57 (br m, 4H), 1.29 (br m, 12H). HRMS: calcd *m*/*z* for $C_{19}H_{38}O_6S$ $(M + H)^+$ 394.2390; found 394.2381.

(b) 29-Mercapto-3,6,9,12,15,18-hexaoxanonacosanoic Acid (EG5-COOH). EG5-COOH was synthesized by the synthetic procedure mentioned above. Penta(ethylene glycol) was used for the synthesis of EG5-COOH instead of tri(ethylene glycol).

^{1}H NMR (300 MHz, $CDCl_3$): δ 4.18 (s, 2H), 3.56 (m, 20H), 3.45 (t, 2H), 2.51 (q, 2H), 1.57 (br m, 4H), 1.29 (br m, 12H). HRMS: calcd *m/z* for $C_{23}H_{46}O_8S$ $(M + H)^+$ 482.2914; found 482.2889.

(c) (1S)-N-(5-Amino-1-carboxypentyl)iminodiacetic Acid (NTA-NH_2). NTA-NH_2 was synthesized by following the reported procedure.[34] In short, N^6-carbobenzyloxy-L-lysine was dissolved in an aqueous NaOH solution (2 N), and the resulting solution was added dropwise to a stirred solution of bromoacetic acid in an aqueous NaOH solution (2 N) at 0 °C. The mixture was stirred at room temperature for 12 h, heated at 80 °C for 2 h, and acidified by 1 N HCl at room temperature. The precipitate was filtered off and dried to afford a white powder. A solution of the white powder in MeOH/H_2O containing 10% Pd/C catalyst was stirred under H_2 for 7 h. After the removal of the catalyst and solvents and the recrystallization, a white crystal was obtained. ^{1}H NMR (300 MHz, D_2O): δ 3.77 (m, 5H), 2.85 (t, 2H), 1.76 and 1.54 (2m, 6H).

(d) 1-Eicosanethiol (C20SH) and 1-Docosanethiol (C22SH). The synthesis of C20SH and C22SH was reported previously.[67] In short, to an argon-purged ethanol in a two-neck flask equipped with a reflux condenser was added thiourea. After the mixture was stirred to dissolve thiourea in ethanol, 1-bromoeicosane or 1-bromodocosane was added and the resulting mixture was heated to reflux for 12 h. The reaction was allowed to cool to room temperature under an argon atmosphere and 10% (w/w) aqueous KOH solution was added. The resulting mixture was heated to reflux for 4 h. The hydrolyzed solution was titrated to about pH 7. After the removal of solvents and column chromatography, colorless liquid was obtained.

Preparation of Gold-Coated Substrates. Gold-coated substrates were prepared by a thermal deposition of a high-purity gold (100 nm) onto single-crystal silicon wafers that had been primed with titanium (5 nm) as an adhesive layer. The gold-coated wafers were stored in a sealed glass and used as soon as possible after being exposed to the atmosphere. Before use, the gold-coated wafers were cut into pieces ($\sim 1 \times 3$ cm) with a diamond-tipped stylus.

Preparation of SAMs. Before the preparation, the gold-coated substrates were thoroughly washed with methylene chloride, acetone, and ethanol, and then dried under a stream of argon to remove contaminants from the substrates. Subsequently, the substrates were placed in a scintillation vial that contained a freshly prepared 1 mM solution of the thiols at room temperature for 12 h. C12SH, C16SH, and C18SH were easily dissolved in absolute ethanol, and C20SH and C22SH were dissolved in absolute ethanol by sonicating the mixture for 30 min. For the carboxylic acid-terminated thiols (C15-COOH, EG3-COOH, and EG5-COOH), a mixture of absolute ethanol, DI water and acetic acid (80:10:10 v/v) was used to prepare the solutions of the thiols. Thicknesses of the unsubstituted thiols were measured to be 11.5 Å (C12SH), 16.7 Å (C16SH), 19.6 Å (C18SH), 21.5 Å (C20SH), and 23.8 Å (C22SH) by ellipsometry. After the formation of SAMs, the substrates were thoroughly rinsed with ethanol, methylene chloride and THF several times, and then dried under a stream of argon.

Coupling Reactions. A gold substrate presenting COOH-terminated SAMs was immersed in a DI water solution of 1-[3-(dimethylamino)propyl]-3-ethylcarbodiimide hydrochloride (EDC) (10 mM) and *N*-hydroxysuccinimide (NHS) (10 mM) for 30 min, washed with 1 mL of DI water, and immersed in a 12 mM phosphate buffered saline (PBS) solution (pH 8.3) of NTA-NH_2 (3 mg/mL) for 12 h. For a complexation of Ni(II) onto the NTA-presenting surface, the substrate was submersed in an 1 mM NaOH solution (pH 11) for 5 min for the deprotonation of carboxylic acid groups and then incubated in an aqueous solution of nickel sulfate ($NiSO_4$, 200 mM) at room temperature for 1 h. The deprotonation step was necessary since the binding of Ni(II) to the NTA group is strongest in alkaline pH.[30]

Polarized Infrared External Reflectance Spectroscopy (PIERS). PIERS spectra were recorded with a nitrogen-purged Thermo Nicolet Fourier transform infrared spectrometer (model: NEXUS). The instrument was equipped with a liquid nitrogen-cooled mercury-cadmium-telluride (MCT) detector and a Smart Apertured Grazing Angle (smart SAGA) apparatus for grazing-angle reflectance IR spectroscopy. The *p*-polarized light was incident at 80° relative to the surface normal of the substrate. The spectra were taken by adding approximately 2000 scans for background and 800−2000 scans for the samples (resolution of 4 cm^{-1}, gain of 4, mirror velocity of 3.1647 cm/s, beam splitter of KBr, aperture of 69), and the final spectra were obtained with minimum of baseline correction. A bare gold was used for obtaining a reference spectrum.

Ellipsometry. Ellipsometric measurements were performed by using a Gaertner Scientific ellipsometer (model: L116s) equipped with a He−Ne laser ($\lambda = 6328$ Å), set at an angle of incidence of 70°. The gold substrate constants were derived from ellipsometric measurements conducted at 10 or more locations on a bare gold substrate. For the substrates coated with SAMs, the thickness of the SAM was determined from ellipsometric measurements at different 3−5 spots (separated by at least 0.5 cm), using the recorded substrate constants and assuming that the refractive index of the film was 1.46 and the film was completely transparent to the laser beam.

X-Ray Photoelectron Spectroscopy (XPS). The XPS spectra were obtained by using a VG-Scientific ESCALAB 250 spectormeter with monocromatized Al Kα X-ray source (1486.6 eV). Emitted photoelectrons were detected by a multichannel detector at a takeoff angle of 90° relative to the surface. During the measurements, the base pressure was 10^{-9}−10^{-10} Torr. Survey spectra (resolution of 1 eV, spot size of 500 μm, 3 scans) and high-resolution spectra of the C 1s, N 1s, O 1s, S 2p, Ni 2p, and Au 4f regions (resolution of 0.05 eV, spot size of 500 μm, 5−20 scans) were obtained. Atomic compositions were determined by using standard multiplex fitting routines with the following sensitivity factors: 1.00 (C 1s), 1.80 (N 1s), 2.93 (O 1s), 1.677 (S 2p), and 14.61 (Ni 2p3/2).[68] All binding energies were determined with the Au 4f7/2 core level peak at 84 eV as a reference.[69] Electron mean free paths for N 1s and S 2p were determined experimentally from a series of SAMs of *n*-alkanethiols $[CH_3(CH_2)_{n-1}SH$, $n = 12, 16, 18, 20, 22]$ on gold by measuring the attenuation of the gold peak (Au 4f) with increasing film thickness, which gave the electron mean free paths as a function of the kinetic energy of the photoelectrons for the region of interest.

Surface Plasmon Resonance (SPR) Spectroscopy. SPR measurements were performed with a Biacore instrument (model: Biacore X). The SAMs terminating in COOH groups were prepared on gold substrates (purchased from K-MAC, Korea), which were prepared by a sequential deposition of titanium (1.5 nm) and gold (39 nm) onto glass cover slips (0.2 mm, No. 2. Corning, reflective index = 1.52). The gold substrates were immersed in an 1 mM solution (EtOH:water:acetic acid = 80:10:10 v/v) of C15-COOH, EG3-COOH, or EG5-COOH for 12 h, rinsed with ethanol, and dried with a stream of argon, followed by the NTA coupling and Ni(II) complexation reactions as mentioned above. The substrates were then washed with DI water and PBS, and they were glued onto Biacore cassettes.

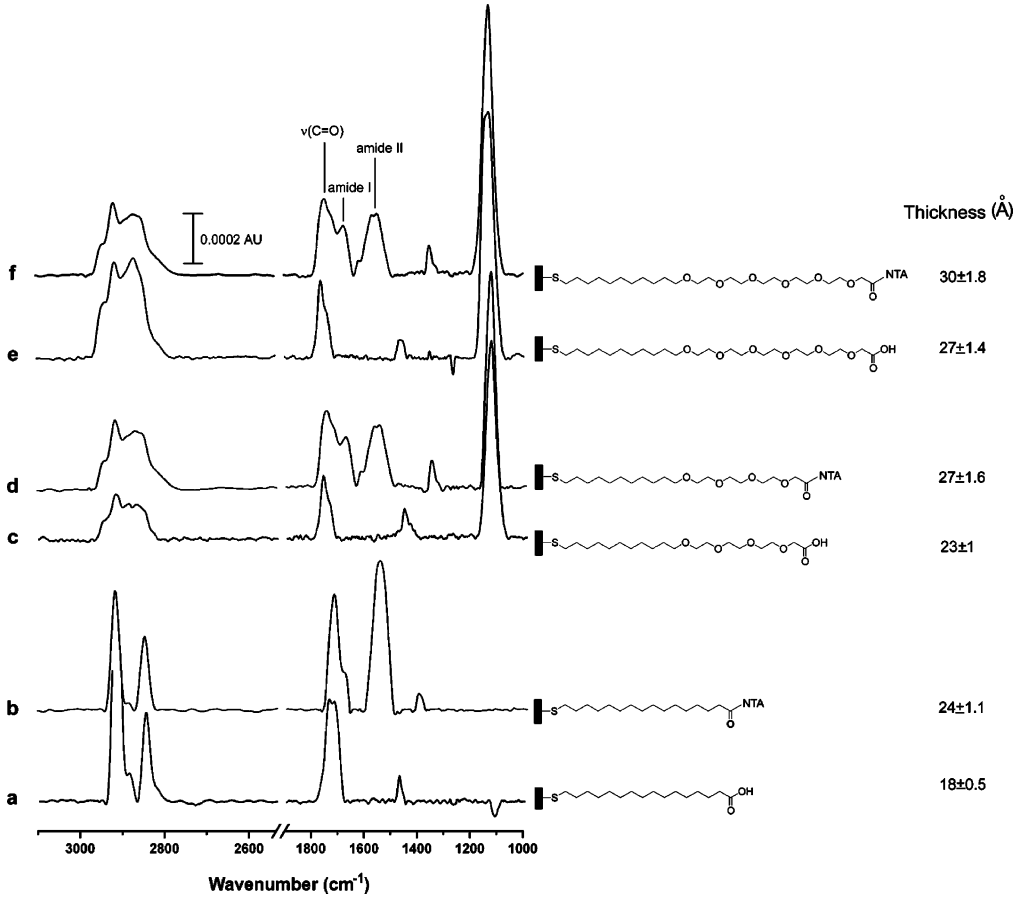

Figure 3. PIERS spectra and ellipsometric thicknesses. (a and b) The SAM of C15-COOH before and after the NTA coupling. (c and d) The SAM of EG3-COOH before and after the NTA coupling. (e and f) The SAM of EG5-COOH before and after the NTA coupling.

Special care was taken to prevent artifacts due to accumulation of air bubbles or contamination. Prior to each set of experiments, the channels of the SPR instrument were cleaned with a solution of sodium dodesyl sulfate (SDS) (BIAdesorb solution 1). SPR experiments were conducted with a constant 5 μL/min flow of solution over the surfaces. Protein binding onto the NTA-Ni-(II)-terminated SAMs was carried out by sequential injections of 35 μL of PBS and 50 μL of a protein solution diluted in PBS (0.1 mg/ mL). After the elution of the protein solution for 10 min, the surface was washed with 50 μL of PBS. Protein binding resulted in a shift in the resonance angle that was reported in resonance units (RU; 10000 RU = 1.0).[27]

Purification of His-Tagged Proteins. The gene encoding enhanced green fluorescent protein (EGFP) was PCR-amplified from pEGFP-c2 (Clontech) and cloned into the NheI and HindIII sites of the *E. coli* expression vector pET28a (Novagen). The resulting construct, pET28a-EGFP, encoded the EGFP protein including an N-terminal His-tag. His-tagged GFP protein was overexpressed in *E. coli* strain BL21 (DE3) (Novagen) as follows: transformants containing pET28a-EGFP were grown at 37 °C in Luria-Bertani medium and induced with 0.5 mM isopropyl-β-D-thiogalactopyranoside (IPTG) at an OD_{600} of 0.8. Cells were harvested after 4-h further incubation at 37 °C. The His-tagged GFP protein was purified essentially to homogeneity by column chromatography. Briefly, the His-tagged GFP protein was bound to a His-bind resin (Novagen) and eluted with 300 mM imidazole. The protein was further purified using a Hi-Trap Q FF column (Amersham). The His-tagged GFP was dialyzed into PBS buffer and concentrated to above 1 mM. The concentration of proteins was determined by the Bradford method.[70]

Results and Discussion

Compounds. Three COOH-terminated SAMs were formed in this study (Figure 1). 16-Mercaptohexadecanoic acid [$HS(CH_2)_{15}COOH$, C15-COOH] was chosen because the SAM of C15-COOH has relatively well been characterized[71−73] and presents a carboxylic acid group at the tail end. We incorporated an ethylene glycol (EG) group into SAM-forming compounds [$HS(CH_2)_{11}(OCH_2CH_2)_3OCH_2COOH$ (EG3-COOH) and $HS(CH_2)_{11}(OCH_2CH_2)_5OCH_2COOH$ (EG5-COOH)] to make the resulting SAMs flexible. In addition to the flexibility, the EG group is known to reduce nonspecific adhesion of biomolecules and cells onto surfaces effectively. A long alkyl chain (i.e., eleven-methylene group) was used for maintaining the integrity of the formed SAMs, and the number of the EG groups was varied to either three or five.

Formation and Characterization of SAMs. The SAMs of C15-COOH, EG3-COOH, and EG5-COOH were formed in an 1 mM solution of each compound composed of absolute ethanol, deionized (DI) water, and acetic acid (80:10:10 v/v). The resulting SAMs were characterized by polarized infrared external reflectance spectroscopy (PIERS), contact angle goniometry, ellipsometry, and X-ray photoelectron spectroscopy (XPS).

The thicknesses of the SAMs were measured to be 18 Å (for C15-COOH), 23 Å (for EG3-COOH), and 27 Å (for EG5-COOH), and water static contact angles were approximately 30° in all the three cases. Characteristic peaks in the IR spectra further confirmed the formation of SAMs terminating in COOH group (Figure 3). The CH_2 stretching vibrations of the alkyl chain are very sensitive to the lateral packing density and to the presence of gauche defects, which makes these vibration modes ideally suited as probes to determine the crystallinity of

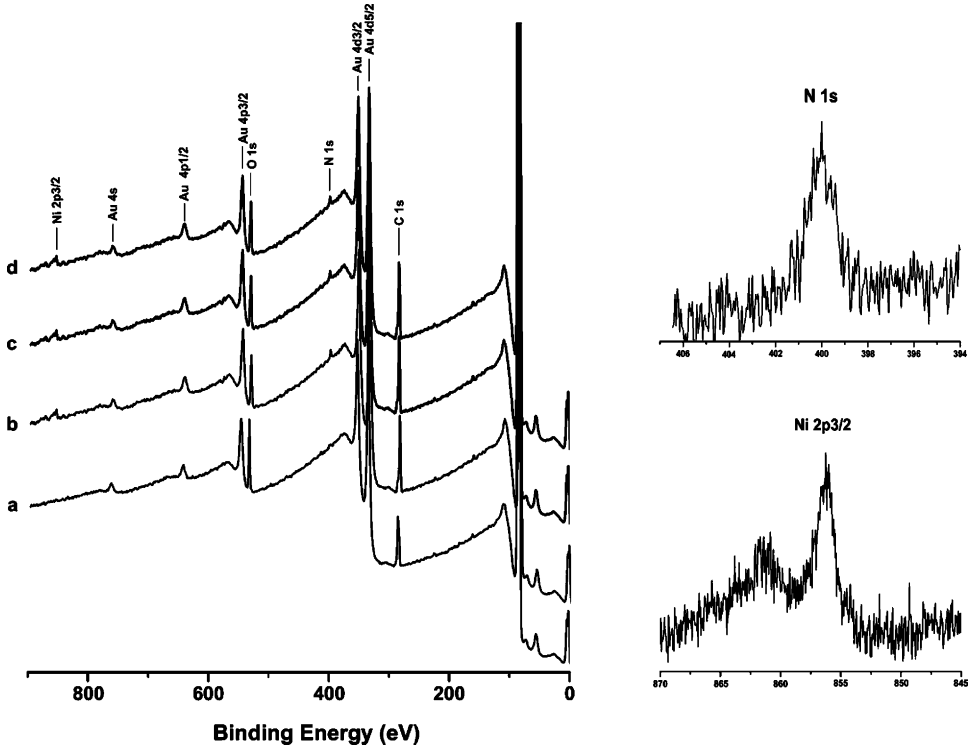

Figure 4. XPS spectra of the SAMs of (a) EG3-COOH, (b) C15-NTA-Ni(II), (c) EG3-NTA-Ni(II) and (d) EG5-NTA-Ni(II). The SAM of C15-NTA-Ni(II) indicates the one after the NTA coupling and Ni(II) complexation onto the SAM of C15-COOH, and the SAM of EG(3 or 5)-NTA-Ni(II) indicates the one after the NTA coupling and Ni(II) complexation onto the SAM of EG(3 or 5)-COOH.

SAMs. In particular, the asymmetric CH_2 stretching vibration is a useful indicator of the cryatallinity of SAMs. For densely packed, crystalline SAMs, the peak of asymmetric CH_2 stretching vibration would appear between 2916 and 2918 cm^{-1}. In the IR spectrum of the SAM of C15-COOH, the CH_2 stretching vibration peaks were observed around at 2848 cm^{-1} (symmetric CH_2 stretching) and 2917 cm^{-1} (asymmetric CH_2 stretching) (Figure 3a). The peak positions of the CH_2 stretching vibration (especially the peak position of the asymmetric CH_2 stretching band at 2917 cm^{-1}) are well in agreement with the peak positions of the CH_2 stretching vibration of the highly crystalline, well-ordered SAM of C15-COOH.[73] The peaks from the COOH group were also observed at 1470 cm^{-1} (COO^-), 1718 cm^{-1} (C═O stretching of acyclic dimers), and 1738 cm^{-1} (C═O stretching of monomers). On the basis of the relative intensity of the peaks, the amount of monomeric carboxylic acids (including the deprotonated carboxylates) was estimated to be roughly 50% in the sample. In the SAMs of EG3-COOH and EG5-COOH, the additional peaks from the EG group were observed at 2870 cm^{-1} (symmetric EG CH_2 stretching) and around at 2930 cm^{-1} (asymmetric EG CH_2 stretching).[74,75] The peak at 1750 cm^{-1} (assigned as C═O stretching of monomers) has a shoulder around at 1736 cm^{-1}. XPS study also confirmed the presence of the SAMs on gold surfaces: the oxygen signal was observed at 531 eV (O 1s) and the carbon signal at 284.6 eV (C 1s) in addition to the gold signals (Figure 4 and the Supporting Information).

Densely packed and defect-free SAMs of alkanethiols with 100% coverage has the lateral packing density of 4.67 molecules/nm^2 on Au(111) surfaces (corresponding to 21.4 $Å^2$ per molecule).[74,76] The effective thicknesses (and the lateral packing densities) of the COOH-terminated SAMs can be calculated by comparing the attenuation of the Au 4f XPS signal by the SAMs of C15-COOH, EG3-COOH, or EG5-COOH with the attenuation of the Au 4f XPS signal by the SAMs of reference

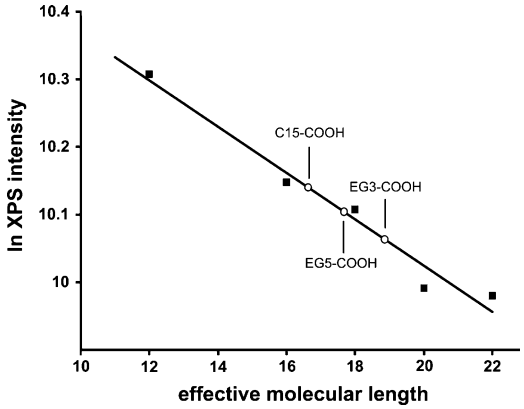

Figure 5. Attenuation of the substrate photoelectron intensity (Au 4f) for unsubstituted alkanethiols with 12, 16, 18, 20, and 22 carbon atoms (C12SH, C16SH, C18SH, C20SH, and C22SH) (closed squares). The effective thicknesses of the SAMs of COOH-terminated thiols (open circles) were determined by using the least-squares fit for the SAMs of unsubstituted alkanethiols as a reference.

alkanethiols. As a reference system, SAMs of unsubstituted alkanethiols (C12SH, C16SH, C18SH, C20SH, and C22SH) were used to determine the attenuation of the Au 4f signals as a function of the effective thickness of the SAMs: the logarithmic Au 4f intensities decreased with increasing the molecular length of the unsubstituted alkanethiols (Figure 5). The least-squares fit for the SAMs of the unsubstituted alkanethiols was used as a reference to determine the effective thicknesses and the lateral packing densities of the COOH-terminated SAMs. The experimental data showed that the attenuation of the Au 4f signal by the SAM of C15-COOH, composed of 16 carbons and 2 oxygens, corresponded to the attenuation of the Au 4f signal by a SAM of C16.6SH, indicating that the SAM of C15-COOH had a relative coverage of 92.4% on Au(111) compared with the SAM of C18SH and a lateral

SCHEME 1: Schematic Description of the Procedure for Immobilization of His-Tagged Proteins[a]

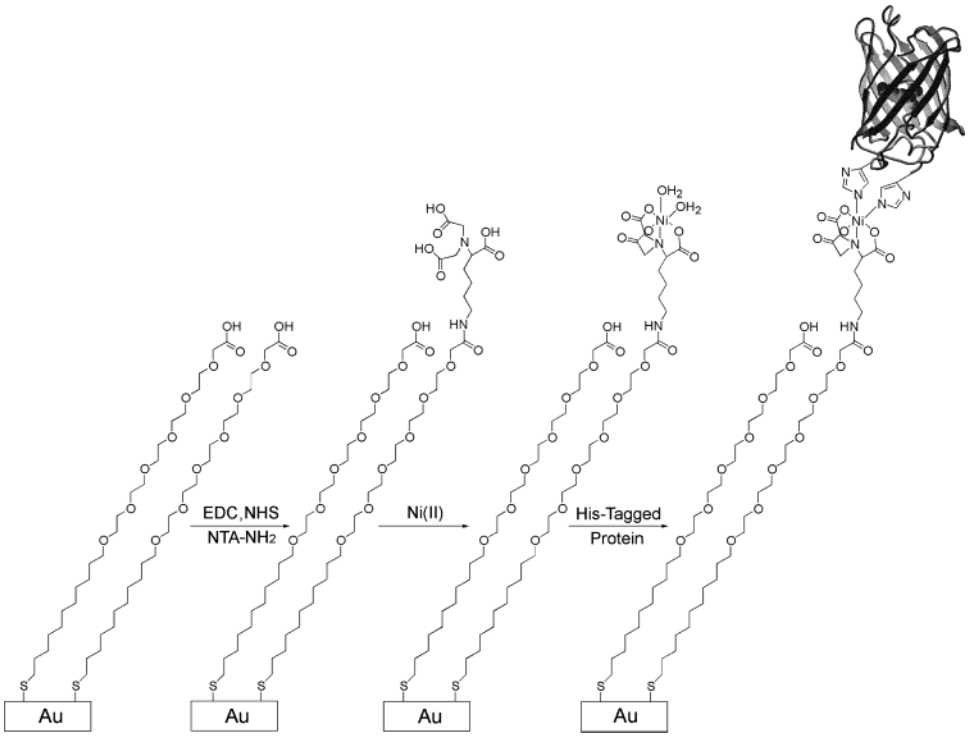

[a] A representative protein (green fluorescent protein; GFP) is shown in the scheme.

packing density of 4.32 molecules/nm^2. In the SAMs containing the EG moiety (EG3-COOH and EG5-COOH), the EG moiety is expected to reduce effective thickness and lateral packing density in comparison with C15-COOH. The attenuation of the Au 4f signal by the SAM of EG3-COOH corresponded to the attenuation by the SAM of 18.7 carbon atoms on average. Therefore, the SAM of EG3-COOH had a coverage of 74.8% relative to an unsubstituted alkanethiol and an average lateral packing density of 3.49 molecules/nm^2. With increasing the number of the EG groups, lower packing density is expected: the experimentally determined effective molecular length of 17.6 for EG5-COOH (corresponding to a lateral packing density of 2.65 molecules/nm^2) was lower than the lateral packing density of the SAM of EG3-COOH.

Coupling Reactions and Characterization. We optimized reaction conditions for the amide coupling between (1S)-*N*-(5-amino-1-carboxypentyl)iminodiacetic acid (NTA-NH_2) and COOH-terminated SAMs, and we monitored the coupling efficiency by PIERS, ellipsometry, and XPS. The maximum coupling was achieved when *N*-hydroxysuccimide (NHS)-activated SAMs were reacted with NTA-NH_2 in a PBS buffer (pH 8.3) for 12 h. The IR spectra of SAMs after the coupling are shown in Figure 3 and the assignments of the important peaks present in the IR spectra are presented in the Supporting Information. Characteristic amide peaks after the coupling appeared around at 1670 cm^{-1} (amide I; C═O stretch) and 1550 cm^{-1} (amide II; N−C═O stretch).[77,78] For example, in the SAM of C15-COOH the amide peaks were observed at 1677 and 1550 cm^{-1} (Figure 3b) and in the SAM of EG5-COOH at 1670 and 1554 cm^{-1} (Figure 3f). The relative intensity of the amide I and amide II peaks provides an insight into the orientation of the amide bond on surfaces. Compared with Figures 3d and f (where the intensity of the amide I peak is approximately the same as that of the amide II peak), Figure 3b shows a relatively weak intensity of the amide I peak at 1677 cm^{-1}. On the basis of the surface selection rule, the observed relative intensities are consistent with the orientation of the amide group with both the C═O and the N−H bonds almost parallel to the surface. In the SAMs of EG3-COOH and EG5-COOH, the flexibility of the EG group and the lower packing density would allow for the random rotation of the amide bond, which generates approximately similar intensities of the amide I and II peaks. Ellipsometric measurements showed that the increase in the film thickness was 6 Å (for C15-COOH), 4 Å (for EG3-COOH), and 3 Å (for EG5-COOH), respectively. We can infer the relative densities of NTA on surfaces from the increased thicknesses: for example, the density of coupled NTA groups on the SAM of C15-COOH would be twice as high as that of coupled NTA groups on the SAM of EG5-COOH.

The coupling was further confirmed by XPS studies. After the coupling, the N 1s peak was observed at 402 eV. Panels b−d of Figure 4 show the XPS spectra of the SAMs of C15-COOH, EG3-COOH, and EG5-COOH after the coupling and a subsequent complexation of Ni(II) onto the NTA group, respectively, and Figure 4a shows the XPS spectrum of the SAM of EG3-COOH before the coupling as a comparison. In addition to the N 1s peak, the appearance of a peak at 856 eV (Ni 2p3/2) confirms the successful coupling of NTA-NH_2 and complexation of Ni(II) onto surfaces. The Ni 2p3/2 high-resolution spectrum (shown in the bottom right of Figure 4) consisted of a main photoemission peak at 856.0 eV along with a broad satellite peak at a 5.6-eV higher binding energy. This spectrum is in agreement with the reported Ni 2p3/2 high-resolution XPS spectrum.[34]

The coupling yields were estimated by analyzing the XPS data.[79] We compared the experimentally determined N 1s to S 2p (N/S) ratio with the N/S ratio calculated for the functionalization of the SAMs presenting NTA-Ni(II). In the SAM of C15-COOH, the experimentally determined N/S ratio (0.63) corresponded to the calculated N/S ratio for the coupling of 30% of the COOH groups (0.65), implying that on average three COOH groups among ten COOH groups participated in the coupling

reaction on the SAM of C15-COOH (See the Supporting Information). On the basis of the calculated packing density of C15-COOH thiols on Au(111) (4.32 molecules/nm^2), we can infer that the lateral packing density of NTA-Ni(II) is approximately 1.30 molecules/nm^2 (or 76.9 Å^2 per molecule). In the SAMs of EG3-COOH and EG5-COOH, the experimentally determined N/S ratios (0.49 for EG3-COOH and 0.47 for EG5-COOH) give the estimated coupling yields of 25%. In the SAM of EG3-COOH, the coupling yield (25%) generates a SAM presenting NTA-Ni(II) with a lateral packing density of 0.873 molecules/nm^2 (or 115 Å^2 per molecule). The coupling on the SAM of EG5-COOH yields a SAM presenting NTA-Ni(II) with a lateral packing density of 0.663 molecules/nm^2 (or 151 Å^2 per molecule). The ratio of the increased thicknesses measured by ellipsometry (2:1.3:1 in the order of C15-COOH, EG3-COOH, and EG5-COOH) closely matched the ratio of the lateral packing densities of NTA-Ni(II). On the basis of the two independently estimated ratios, we can conclude that the ratio of the number of NTA-Ni(II) present on the surface is 2:1.3:1 in the order of C15-COOH, EG3-COOH, and EG5-COOH.

Binding of Histidine-Tagged Proteins. Surface plasmon resonance (SPR) is a powerful technique for investigating interfacial phenomena,[26,77] and we used SPR to study the binding of a His-tagged protein onto NTA-Ni(II)-terminated surfaces.[26,31] As a model system for a His-tagged protein, we used a 30-kDa green fluorescent protein (GFP) with a His-tag at the N-terminus. GFP is in the shape of a cylinder (a diameter of about 30 Å and a length of about 40 Å), comprising 11 strands of β-sheet with an α-helix inside and short helical segments on the ends of the cylinder (See Scheme 1 for a graphical representation of GFP).[50] Figure 6a shows a representative SPR signal where the NTA-Ni(II) group was grafted onto the SAM of EG3-COOH [EG3-NTA-Ni(II)]. The SPR signal shows that the binding requires Ni(II) present on the surface: while we observed ΔRU of 1200 on the NTA-Ni(II)-terminated surface, we observed ΔRU of 105 on the surface that had not been pretreated with Ni(II), NTA-terminated surface (EG3-NTA). The NTA-Ni(II)-terminated surface bound more GFPs than the NTA-terminated surface by more than a factor of 10, and we attribute ΔRU of 105 to nonspecific binding (NSB) of GFPs. An SPR response of 700 RU was reported to correspond to 10-Å-thick protein films with a refractive index of 1.46. According to this approximation, the value of 1200 RU will give a 17-Å-thick GFP film on the surface. The addition of a high concentration of imidazole caused dissociation of the His-tagged GFP from the surface, and the treatment of the GFP-bound surface with 200 mM imidazole in PBS for 5 min led to complete dissociation of the bound GFP [and a partial dissociation of Ni(II)] from the surface (Figure 6b).[26,31] After the removal of Ni(II) by eluting 500 mM EDTA in PBS for 10 min,[26,31] we measured ΔRU value of the NSB of His-tagged GFPs: the value was around 100 RU.

Table 1 shows the ΔRU values in the presence and in the absence (NSB) of Ni(II) on the three different surfaces. Among the three surfaces, EG3-NTA-Ni(II) showed highest binding of GFPs: the binding of GFPs to the EG3-NTA-Ni(II) was twice as much as that of GFPs to the EG5-NTA-Ni(II) and approximately one and a half of the binding to the C15−NTA-Ni(II). All the three surfaces have excessive NTA-Ni(II) groups when considering the packing densities of the NTA-Ni(II) (roughly 100 Å^2 per molecule) and the spatial dimension of GFPs (roughly 1000 Å^2 per protein): we presume the observed maximum binding of GFPs onto the EG3-NTA-Ni(II) might be due to a combination of two factors, density and accessibility

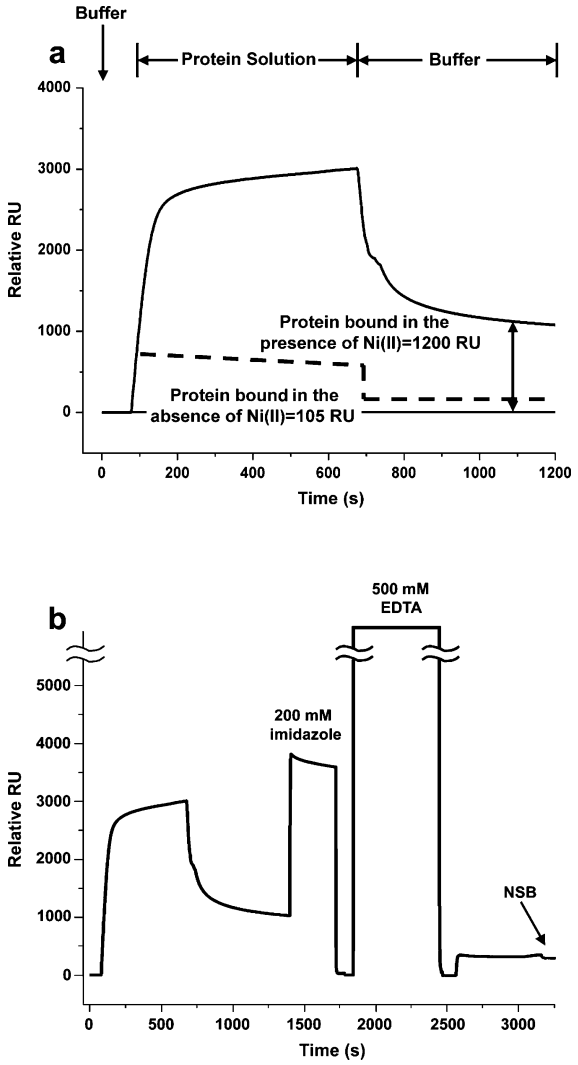

Figure 6. (a) SPR signal on injection of His-tagged GFPs over a SAM presenting EG3-NTA. The solid line is the signal in the presence of Ni(II), and the dashed line is the signal in the absence of Ni(II). (b) SPR signal on binding of His-tagged GFPs onto EG3-NTA-Ni(II) followed by dissociation of the His-tagged GFP with 200 mM imidazole and dissociation of Ni(II) with 500 mM EDTA.

TABLE 1: SPR Signals from Binding of GFPs to Surfaces Presenting NTA Groups in the Presence and in the Absence of Ni(II) and to Surfaces Presenting COOH-Terminated SAMs[a]

	In the Presence of Ni(II)	In the Absence of Ni(II)[b]
C15-NTA	880	140
EG3-NTA	1200	105
EG5-NTA	600	90
		Nonspecific Binding (NSB)[c]
C15-COOH		300
EG3-COOH		10
EG5-COOH		6

[a] Relative resonance unit. [b] Measurements on the surfaces presenting NTA groups before the Ni(II) complexation. [c] Average values from at least three independent measurements.

of the NTA-Ni(II) group. We also observed the effect of the EG groups in minimizing the NSB of proteins onto surfaces. In the absence of Ni(II), all the three surfaces contained the NTA-coupled carboxylic acid and free (uncoupled) carboxylic acid groups, but the surfaces with the EG group (EG3-NTA and EG5-NTA) were more effective in reducing the NSB of

GFPs than the C15-NTA surface. The effect of the EG group on the NSB of GFPs was further investigated by using the SAMs before the amide coupling of NTA-NH_2 (i.e., the SAMs of C15-COOH, EG3-COOH, and EG5-COOH). The bottom table of Table 1 clearly shows the importance of the EG group in reducing the NSB of GFPs: we observed little change (less than 10) in the RU value after flowing a GFP solution and washing with PBS on the surface presenting and EG3-COOH and EG5-COOH (For the SPR signals, see the Supporting Information). In particular, the SAM of EG5-COOH showed a negligible NSB of GFPs onto the surface.

Conclusions

We formed three different COOH-terminated SAMs on Au(111) and characterized them by FT-IR spectroscopy, contact angle goniometry, ellipsometry, and XPS. The SAM of 16-mercaptohexadecanoic acid [$HS(CH_2)_{15}COOH$ (C15-COOH)] showed a well-ordered, highly crystalline structure with a lateral packing density of 4.32 molecules/nm^2 (in comparison, the idealized SAM of alkanethiols has a lateral packing density of 4.67 molecules/nm^2). The structure of the SAM became less ordered (characterized by FT-IR spectroscopy) and the lateral packing density decreased as the ethylene glycol ($HOCH_2CH_2$-OH, EG) group was incorporated into the backbone of alkanethiols as a flexible linker. The estimated lateral packing densities were 3.49 [for the SAM of $HS(CH_2)_{11}(OCH_2CH_2)_3$-$OCH_2COOH$ (EG3-COOH)] and 2.65 molecules/nm^2 [for the SAM of $HS(CH_2)_{11}(OCH_2CH_2)_5OCH_2COOH$ (EG5-COOH)], respectively. Nitrilotriacetic acid (NTA)-containing primary amine [(1S)-*N*-(5-amino-1-carboxypentyl)iminodiacetic acid; NTA-NH_2] was coupled with the carboxylic acid group on surfaces via *N*-hydroxysuccimide (NHS) activation of the carboxylic acid group. The estimated coupling yields (25−30%) were relatively low for all the three surfaces even under the optimized conditions.

SPR studies on the binding of a His-tagged protein onto the surfaces presenting NTA-Ni(II) groups showed that (1) there was an optimal surface density of the NTA-Ni(II) group for a maximum binding of proteins onto surfaces in the oriented way: the surface prepared from EG3-COOH − having a surface density of the NTA-Ni(II) group between those of the surfaces prepared from C15-COOH and EG5-COOH − showed the highest binding of His-tagged GFPs, and (2) the EG group incorporated into the backbone of thiols had some effects in minimizing the nonspecific binding (NSB) of proteins. We observed a greater effect of the EG group of COOH-terminated SAMs in minimizing the NSB of GFPs. More detailed studies on effects of linker flexibility and functionality on the immobilization of proteins and the subsequent protein−protein (protein−ligand) interactions are currently under investigation.

Acknowledgment. This work was supported by the R&D Program for Fusion Strategy of Advanced Technologies. We thank Sangwon Ko and Joon Sung Lee for the experimental assistance and Dr. Won at Korea Basic Science Institute (KBSI) for the XPS analysis. We are also grateful to Mi-Young Hong and Professor Hak-Sung Kim for the SPR measurement.

Supporting Information Available: IR and XPS peak assignments, SPR data, and tables of comparison between the experimentally determined atomic percentages from XPS data and the theoretical values calculated for different coverages. This material is available free of charge via the Internet at http://pubs.acs.org.

References and Notes

(1) Ulman, A. *Chem. Rev*. **1996**, *96*, 1533−1554.
(2) Mrksich, M. *Curr. Opin. Chem. Biol*. **2002**, *6*, 794−797.
(3) Lee, J. K.; Lee, K.-B.; Kim, D. J.; Choi, I. S. *Langmuir* **2003**, *19*, 8141−8143.
(4) Sullivan, T. P.; Huck, W. T. S. *Eur. J. Org. Chem*. **2003**, *1*, 17−29.
(5) Mrksich, M. *Curr. Opin. Colloid Interface Sci*. **1997**, *2*, 83−88.
(6) MacBeath, G.; Schreiber, S. L. *Science* **2000**, *289*, 1760−1763.
(7) Flink, S.; Veggel, F. C. J. M. V.; Reinhoudt, D. N. *Adv. Mater*. **2000**, *12*, 1315−1328.
(8) Lahann, J.; Mitragotri, S.; Tran, T.-N.; Kaide, H.; Sundaram, J.; Choi, I. S.; Hoffer, S.; Somorjai, G. A.; Langer, R. *Science* **2003**, *299*, 371−374.
(9) Kakkar, A. K. *Chem. Rev*. **2002**, *102*, 3579−3588.
(10) Choi, I. S.; Langer, R. *Macromolecules* **2001**, *34*, 5361−5363.
(11) Yoon, K. R.; Lee. K.-B.; Chi, Y. S.; Yun, W. S.; Joo, S.-W.; Choi, I. S. *Adv. Mater*. **2003**, *15*, 2063−2066.
(12) Yoon, K. R.; Chi, Y. S.; Lee, K.-B.; Lee, J. K.; Kim, D. J.; Koh, Y.-J.; Joo, S.-W.; Yun, W. S.; Choi, I. S. *J. Mater. Chem*. **2003**, *13*, 2910−2914.
(13) Mrksich, M.; Whitesides, G. M. *Annu. Rev. Biophys. Biomol. Struct*. **1996**, *25*, 55−78.
(14) Lösche, M. *Curr. Opin. Solid State Mater. Sci*. **1997**, *2*, 546−556.
(15) Turková, J. *J. Chromatogr. B* **1999**, *722*, 11−31.
(16) Zhu, H.; Synder, M. *Curr. Opin. Chem. Biol*. **2003**, *7*, 55−63.
(17) Hearn, M. T. W.; Acosta, D. *J. Mol. Reconit*. **2001**, *14*, 323−369.
(18) Woodbury, C. P.; Venton, D.*J. Chromatogr. B* **1999**, *725*, 113−137.
(19) Herrson, J. N.; Muller, W.; Paudler, M.; Riegler, H.; Ringsdorf, H.; Suci, P. A. *Langmuir* **1992**, *8*, 1413−1416.
(20) Spinke, J.; Liley, M.; Guder, H.-J.; Angermaier, L.; Knoll, W. *Langmuir* **1993**, *9*, 1821−1825.
(21) Pradier, C.-M.; Salmain, M.; Zheng, L.; Jaouen, G. *Surf. Sci*. **2002**, *502−503*, 193−202.
(22) Browning-Kelley, M. E.; Wadu-Mesthrige, K.; Hari, V.; Liu, G. Y. *Langmuir* **1997**, *13*, 343−350.
(23) Delamarcje, E.; Sundarababu, G.; Biebuyck, H.; Michel, B.; Gerber, C.; Sigrist, H.; Ringsdorf, W. H.; Xanthopoulos, N.; Mathieu, H. J. *Langmuir* **1996**, *12*, 1997−2006.
(24) Zhou, D.; Wang, X.; Birch, L.; Rayment, T.; Abell, C. *Langmuir* **2003**, *19*, 10557−10562.
(25) Frecerix, F.; Bonroy, K.; Laureyn, W.; Reekmans, G.; Campitelli, A.; Dejaen, W.; Maes, G. *Langmuir* **2003**, *19*, 4351−4357.
(26) Sigal, G. B.; Bamdad, C.; Barberis, A.; Strominger, J.; Whitesides, G. M. *Anal. Chem*. **1996**, *68*, 490−497.
(27) Keller, T. A.; Duschl, C.; Kröger, D.; Sévin-Landais, A.-F.; Vogel, H.; Cervigni, S. E.; Dumy, P. *Supramol. Sci*. **1995**, *2*, 155−160.
(28) Chen, H.-M.; Luo, S.-L.; Chen, K.-T.; Lii, C.-K. *J. Chromatogr. A* **1999**, *852*, 151−159.
(29) Rigler, P.; Ulrich, W.-P.; Hoffmann, P.; Mayer, M.; Vogel, H. *ChemPhysChem* **2003**, *4*, 268−275.
(30) Thomson, N. H.; Smith, B. L.; Almqvist, N.; Schmitt, L.; Kashlev, M.; Kool, E. T.; Hansma, P. K. *Biophys. J*. **1999**, *76*, 2421−2431.
(31) Schmitt, L.; Dietrich, C.; Tampè, R. *J. Am. Chem. Soc*. **1994**, *116*, 8485−8491.
(32) Thess, A.; Hutscjernreiter, S.; Hoffmann, M.; Tampé, R.; Barmeister, W.; Guckenberger, R. *J. Biol. Chem*. **2002**, *277*, 36321−36328.
(33) Kröger, D.; Liley, M.; Schiweck, W.; Skerra, A.; Vogel, H. *Biosens. Bioelectron*. **1999**, *14*, 155−161.
(34) Roure, O. D.; Debiemme-Chouvy, C.; Malthête, J.; Silberzan, P. *Langmuir* **2003**, *19*, 4138−4143.
(35) Schmid, E. L.; Keller, T. A.; Dienes, Z.; Vogel, H. *Anal. Chem*. **1997**, *69*, 1979−1985.
(36) Hodneland, C. D.; Lee, Y.-S.; Min, D.-H.; Mrksich, M. *Proc. Natl. Acad. Sci. U.S.A.* **2002**, *99*, 5048−5052.
(37) Wang, D.; Liu, S.; Trummer, B. J.; Deng, C.; Wang, A. *Nat. Biotechnol*. **2002**, *20*, 275−281.
(38) Horan, N.; Yan, L.; Isobe, H.; Whitesides, G. M. *Proc. Natl. Acad. Sci. U.S.A.* **1999**, *96*, 11782−11786.
(39) Wood, L. L.; Cheng, S.-S.; Edmiston, P. L.; Saaverdra, S. S. *J. Am. Chem. Soc*. **1997**, *119*, 571−576.
(40) Bieri, C.; Ermst, O. P.; Heyse, S.; Hofmann, K. P.; Vogel, H. *Nat. Biotechnol*. **1999**, *17*, 1105−1108.
(41) Madoz, J.; Kuznetzov, B. A.; Medrano, F. J.; Garcia, J. L.; Fernandez, V. M. *J. Am. Chem. Soc*. **1997**, *119*, 1043−1051.
(42) Blawas, A. S.; Reichert, W. M. *Biomaterials* **1998**, *19*, 595−609.
(43) Prime, K. L.; Whitesides, G. M. *Science* **1991**, *252*, 1164−1167.
(44) Prime, K. L.; Whitesides, G. M. *J. Am. Chem. Soc*. **1993**, *115*, 10714−10721.

(45) Duvel, R. V.; Corn, R. M. *Anal. Chem.* **1992**, *64*, 337−342.
(46) Sortino, S.; Petralia, S.; Conoci, S.; Bella, S. D. *J. Am. Chem. Soc*. **2003**, *125*, 1122−1123.
(47) Yan, L.; Marzolin, C.; Terfort, A.; Whitesides, G. M. *Langmuir* **1997**, *113*, 66704−66712.
(48) Ostuni, E.; Chapman, R. G.; Holmlin, R. E.; Takayama, S.; Whitesides, G. M. *Langmuir* **2001**, *17*, 5605−5620.
(49) Hyun, J.; Chilkoti, A. *Macromolecules* **2001**, *34*, 5644−5652.
(50) Schmid, E. L.; Keller, T. A.; Cienes, Z.; Vogel, H. *Anal. Chem*. **1997**, *69*, 1979−1985.
(51) Frey, B. L.; Corn, R. M. *Anal. Chem.* **1996**, *68*, 3187−3193.
(52) Cooper, M. A.; Fiorini, M. T.; Abell, C.; Williams, D. H. *Bioorg. Med. Chem.* **2000**, *8*, 2609−2616.
(53) Pirrung, M. C. *Angew. Chem., Int. Ed*. **2002**, *41*, 1276−1289.
(54) Pardo, L.; Wilson, W. C.; Boland, T. J. *Langmuir* **2003**, *19*, 1462−1466.
(55) MacBeath, G.; Schreiber, S. L. *Science* **2000**, *289*, 1760−1763.
(56) Xia, Y.; Whitesides, G. M. *Angew. Chem., Int. Ed.* **1998**, *37*, 550−575.
(57) Li, H.-W.; Muir, B. V. O.; Fichet, G.; Huck, W. T. S. *Langmuir* **2003**, *19*, 1963−1965.
(58) Odom, T. W.; Thallade, V. R.; Love, J. C.; Whitesides, G. M. *J. Am. Chem. Soc*. **2002**, *124*, 12112−12113.
(59) Li, H.-W.; Kang, D.-J.; Blamire, M. G.; Huck, W. T. S. *Nano Lett.* **2002**, *2*, 347−349.
(60) Lee, K.-B.; Park, S.-J.; Mirkin, C. A.; Smith, J. C.; Mrksich, M. *Science* **2002**, *295*, 1702−1705.
(61) Agarwal, G.; Naik, R. R.; Ostone, M. O. *J. Am. Chem. Soc.* **2003**, *125*, 7408−7412.
(62) Hong, S.; Zhu, J.; Mirkin, C. A. *Science* **1999**, *286*, 523−525.
(63) Wadu-Mesthrige, K.; Amro, N. A.; Garno, J. C.; Xu, S.; Liu, G.-Y. *Biophys. J*. **2001**, *80*, 1891−1899.
(64) Hochuli, E.; Döbeli, H.; Schacher, A. *J. Chromatogr*. **1987**, *411*, 177−184.
(65) Luk, Y.-Y.; Tingey, M. L.; Hall, D. J.; Israel, B. A.; Murphy, C. J.; Bertics, P. J.; Abbott, N. L. *Langmuir* **2003**, *19*, 1671−1680.
(66) Zhu, H.; Bilgin, M.; Bangham, R.; Hall, D.; Casamayor, A.; Bertone, P.; Lan, N.; Jansen, R.; Bidlingmaier, S.; Houfek, T.; Mitchell, T.; Miller, P.; Dean, R. A.; Gerstein. M.; Snyder, M. *Science* **2001**, *293*, 2101−2105.
(67) Peanasky, J. S.; McCarley, R. L. *Langmuir* **1998**, *14*, 113−123.
(68) Scofield, J. H. *J. Electron Spectrosc*. **1976**, *8*, 129−137.
(69) Cecchet, F.; Pilling, M.; Hevesi, L.; Schergna, S.; Wong, J. K. Y.; Clarkson, G. J.; Leigh, D. A.; Rudolf, R. *J. Phys. Chem. B* **2003**, *107*, 10863−10872.
(70) Bradford, M. M. *Anal. Biochem.* **1976**, *72*, 248−254.
(71) Bain, C. D.; Troughton, E. B.; Tao, Y. T.; Evall, J.; Whitesides, G. M.; Nuzzo, R. G. *J. Am. Chem. Soc*. **1989**, *111*, 321−335.
(72) Nuzzo, R. G.; Dubois, L. H.; Allara, D. L. *J. Am. Chem. Soc*. **1990**, *112*, 558−569.
(73) Arnold, R.; Azzam, W.; Terfort, A.; Wöll, C. *Langmuir* **2002**, *18*, 3980−3992.
(74) Harder, P.; Grunze, M.; Dahint, R.; Whitesides, G. M.; Laibinis, P. E. *J. Phys. Chem. B* **1998**, *102*, 426−436.
(75) Pale-Grosdemange, C.; Simon, E. S.; Prime, K. L.; Whitesides, G. M. *J. Am. Chem. Soc*. **1991**, *113*, 12−20.
(76) Herrwerth, S.; Eck, W.; Reinhardt, S.; Grunze. M. *J. Am. Chem. Soc.* **2003**, *125*, 9359−9366.
(77) Lahiri, J.; Isaacs, L.; Tien, J.; Whitesides, G. M. *Anal. Chem*. **1999**, *71*, 777−790.
(78) Jordan, C. E.; Frey, B. L.; Kornguth, S.; Corn, R. M. *Langmuir* **1994**, *10*, 3642−3648.
(79) Uvdal, K.; Petoral, R. M. *J. Phys. Chem. B* **2003**, *107*, 13396−13402.